Math. Model. Nat. Phenom.
Vol. 6, No. 3, 2011, pp.166-188
DOI: 10.1051/mmnp/20116307

Automated CFD Analysis for the Investigation of Flight Handling Qualities

M. Ghoreyshi[1*], K. J. Badcock[1], A. Da Ronch[1], D. Vallespin[1]
A. Rizzi [2]

[1] School of Engineering, University of Liverpool, Liverpool, UK, L69 3GH
[2] Aeronautical and Vehicle Engineering, Royal Institute of Technology (KTH), SE-100 44, Sweden

Abstract. Physics based simulation is widely seen as a way of increasing the information about aircraft designs earlier in their definition, thus helping with the avoidance of unanticipated problems as the design is refined. This paper reports on an effort to assess the automated use of computational fluid dynamics level aerodynamics for the development of tables for flight dynamics analysis at the conceptual stage. These tables are then used to calculate handling qualities measures. The methodological questions addressed are a)geometry and mesh treatment for automated analysis from a high level conceptual aircraft description and b) sampling and data fusion to allow the timely calculation of large data tables. The test case used to illustrate the approaches is based on a refined design passenger jet wind tunnel model. This model is reduced to a conceptual description, and the ability of this geometry to allow calculations relevant to the final design to be drawn is then examined. Data tables are then generated and handling qualities calculated.

Key words: CFD, handling qualities, aircraft design, sampling and data fusion
AMS subject classification: 65Z05, 76M99, 76H99

*Corresponding author, E-mail: m.ghoreyshi@liv.ac.uk

Nomenclature

Symbols

A	wing area
AR	wing aspect ratio
d_v	fuselage maximum cross-section height
$C_{l\beta}$	rolling moment coefficient slope with respect to angle of sideslip
C_{Lq}	lift pitch rate derivative
$C_{m\alpha}$	pitching moment coefficient with angle of attack
$C_{n\beta}$	yawing moment coefficient with side-slip angle
$C_{n\delta_r}$	yawing moment rudder control derivative
$C_{y\beta}$	side force coefficient slope with respect to angle of sideslip
C_L, C_D, C_m	lift, drag and pitching moment coefficients
C_Y, C_l, C_n	side-force, rolling and yawing moment coefficients
Cp	pressure coefficient
K_{wbi}	wing-body interference factor
t/c_m	the mean thickness to chord ratio

Greek

$\Lambda_{\text{C/4}}$	quarter-chord sweep angle
Λ_{LE}	leading-edge sweep angle
Γ	dihedral angle

Subscripts

$fuse$	Fuselage
w	wing

Abbreviations

AC	Aerodynamic Centre
API	Application Programming Interface
CAD	Computer Aided Design
CAE	Computer Aided Engineering
CFD	Computational Fluid Dynamics
CG	Centre of Gravity
EIF	Expected Improvement Function
FHQ	Flight Handling Qualities
MSE	Mean Square Error
RANS	Reynolds Averaged Navier-Stokes

1. Introduction

A prerequisite for the realistic prediction of the flight dynamic behaviour of an aircraft is the availability of complete and accurate aerodynamic data. Traditionally, wind-tunnel measurements are used to fill look-up tables of aerodynamic forces and moments related to the flight state. Wind-tunnel models only become available late in the design cycle and most data at the conceptual design stage relies on handbook methods or linear fluid mechanics assumptions [20, 25, 29]. These methods provide low cost reliable data only for conventional aircraft in aerodynamically benign regions of the flight envelope. However, current trends in aircraft design towards novel shapes, augmented-stability and expanded flight envelopes require a more accurate description of the flight-dynamic behaviour of the aircraft. This provides motivation to move towards Computational Fluid Dynamics(CFD) simulations based on the state-of-the-art computer-aided concept designs since these, in principle have no limitations related to geometry. At the highest practical level, simulation based on the Reynolds Averaged Navier-Stokes(RANS) equations have the potential to predict the full range of regimes of interest to the designer. The current state-of-art in the use of CFD for aircraft design is the generation of data for aerodynamic loads [4]. A number of problems need to be addressed for the routine use of CFD for conceptual design, including the cost of generation of large data tables [13] and the automated handling of geometry [5].

In order to support an automated CFD aircraft design, three procedures need to be considered: geometry definition/mesh generation, the flow simulation and the exploitation of the engineering data from the flow solver output for some design objective. Most dedicated aircraft conceptual design packages construct a simple 3D aircraft model by geometrical lofting techniques. However, these tools do not allow construction of a computational mesh for analysis methods without extensive re-formatting and Computer Aided Design (CAD) repair [17]. In contrast, a disadvantage of a CAD-based geometry model is that generated spline surfaces do not correspond to the parameters that a designer uses to describe the conceptual aircraft geometry (such as wing sweep or thickness) [28]. Some alternatives to CAD are aircraft geometry tools such as Boeing's proprietary tool, General Geometry Generator[8], NASA's Rapid Aircraft Modeler [23, 11], KTH (Royal Institute of Technology)'s CADac [5], Stanford's AEROSURF[1] and KTH's Surface Modeler [†]. Boeing's GGG software, written in the Python language, has a library of lofting codes to create a parameterized geometry model for conceptual aircraft design. NASA's RAM generates a geometry model and a surface mesh from aircraft parameters such as wing aspect ratio, taper ratio, span and angles of twist, sweep, dihedral, etc. The CADac and AEROSURF software are CAPRI-based applications that link the CAD package and the aircraft design software that requests the variation in the geometry. CAPRI (Computational Analysis Programming Interface) [14] offers a coupling to any supported CAD package by using API to access the geometry and topological data [1]. In

[†]http://www.larosterna.com/sumo.html

this paper, the SUMO code is used for geometry definition/mesh generation. Further information is given below.

Historically, many aircraft projects experience problems associated with flight handling qualities, an aircraft attribute that addresses the ability to initiate and subsequently maintain a manoeuvre based on pilot opinion [24]. In the current paper we focus on automating the computational generation of aerodynamic data and its impact on Handling Qualities(HQ) assessment at the conceptual design stage. Three geometry related issues must be considered when applying CFD to conceptual design for handling qualities assessment: The first is, can meshes be generated automatically and calculations run fast enough (to be consistent with use by a designer operating on a short timescale, rather than a CFD specialist on a longer scale)? The second is related to the impact of geometry on the flow predictions. Some aerodynamic phenomena are very sensitive to geometry. As an example, the drag can be significantly increased by wing-fuselage junction separations, and attention to blending to avoid these is a detailed design task which would not be done at the conceptual stage. The level of geometry at the conceptual stage would be likely to promote junction separations that would be predicted by a RANS simulation. In this sense high fidelity simulations on low fidelity geometries may provide misleading information about the underlying properties of the design. The third issue is concerned with the linking of different analysis codes and whether the aerodynamic calculations can be done rapidly enough to be practical.

Considering the first issue, the current state of the art in mesh generation does not routinely allow automatic generation of meshes for RANS simulations around full aircraft configurations [3, 18], although progress is being made in this direction [19] . It is however possible to generate unstructured meshes for Euler simulations automatically. As a step in the direction of using RANS for the automated investigation of handling qualities, it therefore seems practical to develop methods based on the Euler equations.

To investigate the issue of geometry fidelity, the following approach is taken. We start with the DLR F12 wind tunnel model [22]. This is a refined design of a development model for a large passenger jet, featuring an advanced aerofoil section, a fuselage-wing junction blending, twist and dihedral of the wings, and a realistic fuselage. This geometry has been simplified consistent with conceptual aircraft design. A number of investigations relating to the influence of geometry and aerodynamic model level are then carried out to see what can be learned from the simplified geometries, and how representative the lessons are of the final refined design.

The prerequisites of assessing handling qualities are the estimation of mass, centre of gravity, moments of inertia and aerodynamic coefficients for each point in the configuration/flight design space[21]. Such a database could require on the order of 30,000 solutions [27]. At the present time, it is impossible to apply CFD for this number of simulations in a time consistent with design methodology. Fortunately, methods are available that can reduce the computational cost [13].

The paper continues with a description of the geometry handling and the prediction tools. The test case, geometry definition and mesh generation are then detailed. A validation of the aerodynamic tools is made against wind tunnel data. Then, a design study, going from a conceptual geometry description to flight handling quality values in an automated fashion is demonstrated.

2. Computational Tools

2.1. Geometry

For a computer-aided analysis and optimization, the geometry of the initial concept must be described. The Computerized Environment for Aircraft Synthesis and Integrated Optimization Methods (CEASIOM) [16], the design code used in the current paper, incorporates a parameterized description of the geometry, named in this paper the XML-aircraft. Its basic parameters for describing lifting surfaces are: the wing area (A); leading edge sweep (Λ_{LE}) and quarter-chord sweep ($\Lambda_{\mathrm{C/4}}$); aspect ratio (AR); taper ratio; dihedral (Γ), the mean thickness to chord ratio (t/c_m) and the aerofoil section. The definition covers cranked lifting surfaces and any number of LE and TE moving devices. The fuselage consists of a three-segment body. The centre body is assumed to have a constant cross-section symmetric about the x-z plane. An ovoid cross section is described by a distortion coefficient ($0 < \xi_x < 1$), where $\xi_x = 0.5$ shows a circular cross section [15]. The XML-aircraft also includes definitions of wing-fuselage fairing, ventral fin, engines, fuel tanks, baggage hold and cabin dimensions. In summary, the XML-aircraft model is defined by around 100 parameters.

The aerodynamic module in CEASIOM converts the XML-aircraft description into the native geometry format for the aerodynamic prediction tools. Of particular interest is the approach used to automatic mesh generation for the Euler solver. The surface modeling package, SUMO, produces a surface model, and its triangulation. The model can be passed to an extended CAD system or mesh generator as a standard CAD interface file, and the surface mesh direct to a tetrahedral volume mesh generator. The parametrization can be extended to the model in the external CAD system through the CADac/CAPRI tools [5].

SUMO [‡] is a rapid geometry modeling tool for parametrically-defined aircraft configurations. The code, written in C++ , has a library of geometric primitives based on B-spline curves and surfaces to create a parameterized watertight surface model of the complete XML-aircraft. The automatic mesh generation tool in SUMO provides an unstructured surface mesh. The mesh control parameters are estimated from the model geometrical features, such as radii of curvature and the presence of sharp edges. From the surface mesh, unstructured volume meshes can be automatically generated using the tetrahedral mesh generator TetGen [§].

2.2. Flow Simulation

2.2.1. Semi-Empirical Methods

The Data Compendium (DATCOM) is a document of more than 1500 pages covering detailed methodologies for determining stability and control characteristics of a variety of aircraft configurations. In 1979, DATCOM was programmed in Fortran and renamed the USAF stability and control digital DATCOM. Digital DATCOM is a semi-empirical method which produces rapidly the aerodynamic derivatives based on geometry details and flight conditions. DATCOM was primarily

[‡] http://www.larosterna.com/sumo.html
[§] http://tetgen.berlios.de/

developed to estimate aerodynamic derivatives of conventional configurations [26, 30], and, DATCOM methods are not not likely to be accurate or available for non-conventional designs. Other DATCOM limitations are discussed in Reference [7]. Digital DATCOM has been implemented into CEASIOM to run directly from the XML aircraft data.

2.2.2. CFD Methods

Edge [10] is a parallelized CFD package developed by Swedish Defence Research Agency, FOI. The code can be applied to 2D/3D viscous(RANS) or inviscid(Euler), compressible flow problems on unstructured grids with arbitrary elements and is used in Euler mode in CEASIOM. Also, Edge allows both steady state and time accurate calculations.

The space discretisation exploits a node-centred finite-volume technique using an edge based data structure. The computational elements are a set of non-overlapping cells formed as the dual of the primary tetrahedral mesh. Explicit Runge-Kutta time stepping integrates the discrete equations in time. Accelerated convergence to steady state is promoted using agglomeration multigrid and implicit residual smoothing. A Matlab interface allows Edge calculations to be prepared and run from CEASIOM. This call runs the preprocessing routines, launches the calculation and processes the flow solution for the forces and moments.

CEASIOM also provides the possibility to exploit external CFD codes. The example code used in the current work is the Parallel Multiblock Code (PMB)[2]. The Euler and RANS equations are discretised on curvilinear multi-block body conforming grids using a cell-centred finite volume method which converts the partial differential equations into a set of ordinary differential equations. The convective terms are discretised using Osher's upwind method. Monotone Upwind Scheme for Conservation Laws (MUSCL) variable extrapolation is used to provide second-order accuracy with the Van Albada limiter to prevent spurious oscillations around shock waves. The spatial residual is modified by adding a second order discretisation of the real time derivative to obtain a modified steady state problem for the flow solution at the next real time step, which is solved through pseudo time. This pseudo time problem is solved using an unfactored implicit method, based on an approximate linearisation of the residual. The linear system is solved in unfactored form using a Krylov subspace method with Block Incomplete Upper Lower (BILU) preconditioning. The preconditioner is decoupled between blocks to allow a high efficiency on parallel computers with little detriment to the convergence of the linear solver. For the Jacobian matrix of the CFD residual function, approximations are made which reduce the size and improve the conditioning of the linear system without compromising the stability of the time marching. Given a block structured mesh, CEASIOM can prepare input files and launch calculations using PMB.

2.3. Force and Moment Generation Using Sampling and Data Fusion

The aerodynamic prediction methods are used to generate tables of forces and moments for a set of aircraft states (e.g. aircraft angle of attack, side-slip angle, control deflections and etc.), which spans the flight envelope. This potentially entails a large number of calculations, which will be

a particular problem due to the computational cost if CFD is the source of the data. This issue has been addressed by sampling and reconstruction based on Kriging interpolation model and data fusion using Co-Kriging as described in reference [13].

Two scenarios were considered, based on (1) a requirement for tables for a completely new design and (2) for updating tables for an existing design which is being altered. In the first scenario it is assumed that a high fidelity model is required and that this can be generated without user intervention. The emphasis is on a sampling method which will identify nonlinearities in the force and moment tables. Approaches to the sampling based on the Mean Squared Error (MSE) criterion of Kriging and the Expected Improvement Function (EIF) were considered in reference [13].

The second scenario has a designer involved in an interactive session. It is assumed that the aircraft geometry is incremented from an initial design, perhaps selected from a library, and that a high fidelity model is available for the initial design from the first scenario. Data fusion based on Co-Kriging is then used to update this initial model, based on a small number of calculations at an acceptable cost (which at present rules out RANS). In this scenario it is assumed that the main flow features present for the initial geometry are not changed appreciably by the geometry increments. If this is not the case, for example if the wing sweep angle increases so that vortical flow starts to dominate, then either a new initial geometry needs to be selected, or the interactive session needs to be suspended so that a new high fidelity model can be generated under the first scenario.

Using these techniques it was shown that tables which are practically useful could be generated in the order of 100 calculations under the first scenario and 10 calculations under the second scenario.

2.4. Flight Handling Quality Calculation

Flight handling quality deals with the ease and precision of aircraft response to pilot commands. This response is a combination of the short and long term motions. The longitudinal short and long term responses to pitch control are named the Short-period and Phugoid, respectively. These are characterized by the undamped natural frequency (ω), damping ratio (ζ) and time to half amplitude ($T_{\theta 2}$). These values need to provide a balance of control power and dynamic stability of aircraft.

The Simulation and Dynamic Stability Analyzer (SDSA) code [12] is used in this paper. For the assessment of handling qualities, SDSA linearizes the rigid-aircraft equations of motion in the matrix form around the equilibrium (trim) point. The eigenvalues and eigenvectors of the Jacobian matrix are next computed in order to identify the typical modes of the aircraft response and quantify their characteristics. The quality of each response based on pilot evaluations can be deduced using figures of merit given by airworthiness regulations. Cooper[9] introduced a ranking system to express the aircraft handling qualities.

3. Geometry and Meshes

3.1. Configuration

The configuration used in the current paper for testing is based on the F12 wind tunnel model from the German Aerospace Center (DLR). The aircraft layout is shown in Figure 1. The model is a 1:40 scale development model of a passenger jet. The CAD model includes a detailed blend at the wing root and an advanced supercritical aerofoil section. The model was tested by DLR to provide static and dynamic data for the purpose of benchmarking the aerodynamic modules of CEASIOM. This geometry is referred to as the wind tunnel (WT) geometry in this paper.

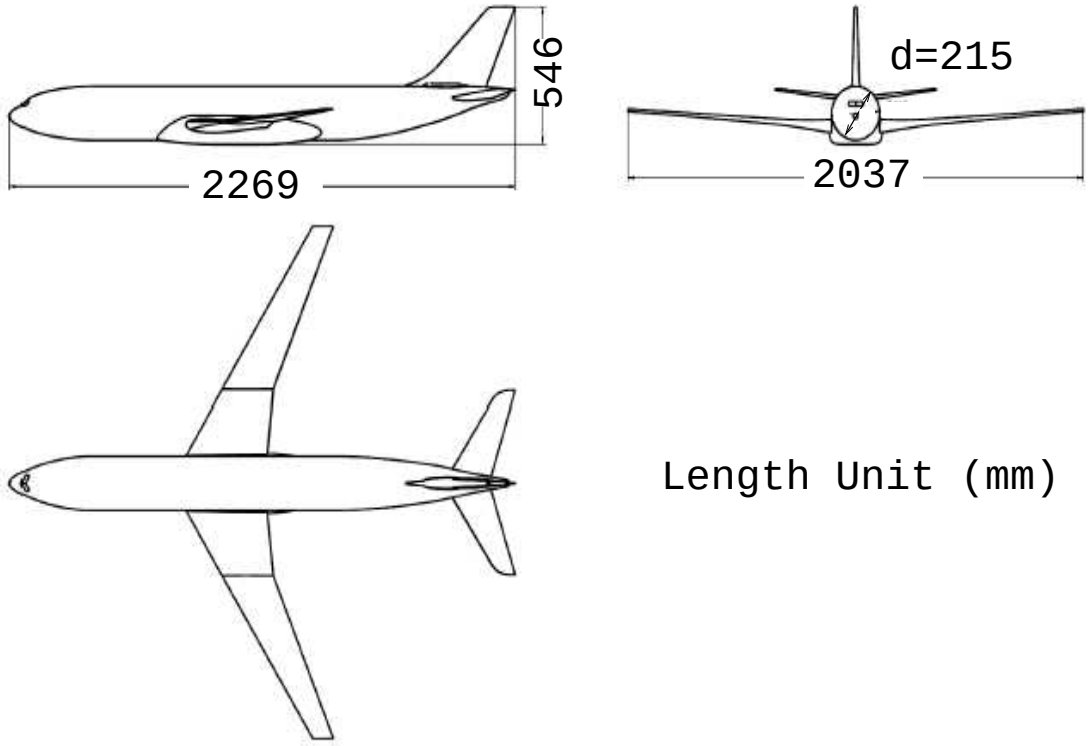

Figure 1: Three View of DLR-F12 [22]

3.2. Geometry Simplification

Based on the detailed CAD model of the WT geometry, the XML aircraft description was produced, referred to as XML1. From this XML description the CAD model was automatically constructed using SUMO. This has a generic aerofoil section and lacks refinements like the fuselage/ wing junction blending, and is meant to represent the detailed design as it would have been during the conceptual phase. In particular, there is a sharp transition from the nose to mid fuselage sections for the XML geometry (Figs. 2-a,2-b). Also, the XML fairing lacks the detailed WT design (Figs. 2-g,2-h). The XML wing, tail and fin tips are not rounded as in the original design. Also, there is no dorsal fin section model in the XML files (Figs. 2-e,2-f).

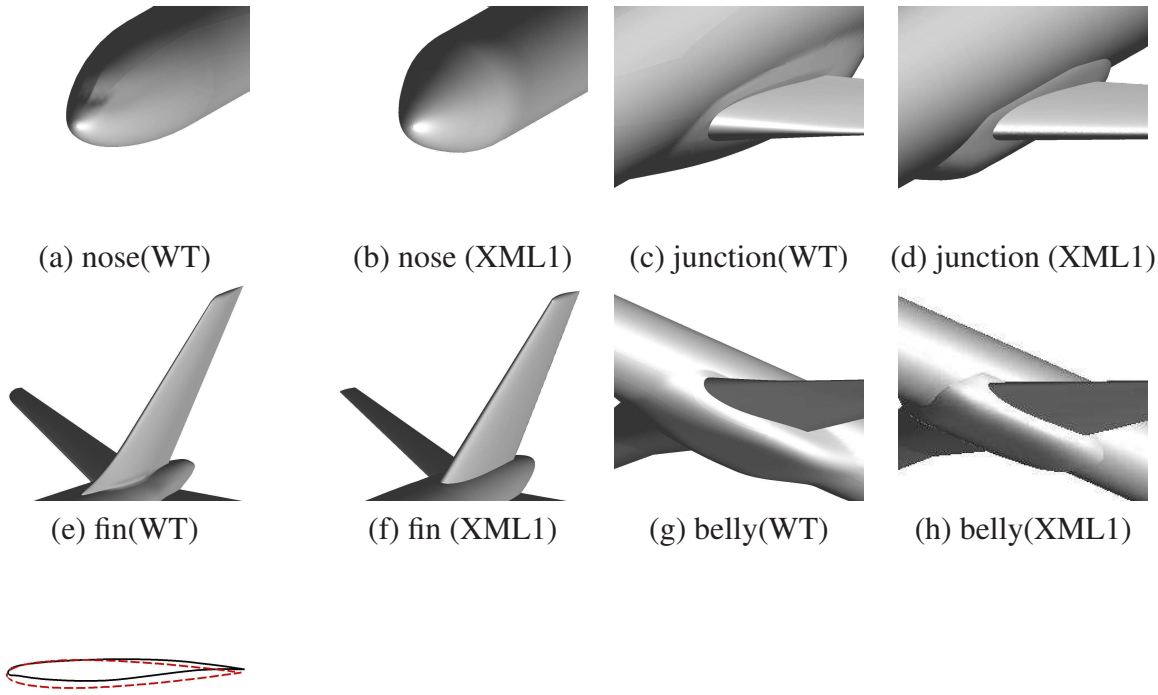

(a) nose(WT) (b) nose (XML1) (c) junction(WT) (d) junction (XML1)

(e) fin(WT) (f) fin (XML1) (g) belly(WT) (h) belly(XML1)

(i) Wing mid-section aerofoil

Figure 2: Details of Comparison of WT and XML aircraft geometries. In subfigure (i), the solid line shows the WT section

3.3. Mesh Generation

Multiblock structured Euler and RANS grids were available for the WT geometry. The Edge meshes were generated automatically by SUMO for the XML geometry. The grid sizes are shown in table 1, and views of the two types of grid in Fig. 3. Comparison of the predictions of the lift,

drag and pitching moment coefficients on the coarse and fine XML1 grids are also shown, and based on this comparison, the coarse grid is used for subsequent calculations.

Table 1: Grids Sizes

Case	Geometry	Number of Grid Points
Euler Half Configuration Coarse	WT	299,320
Euler Half Configuration Fine	WT	2,024,772
RANS Half Configuration Coarse	WT	1,573,470
RANS Half Configuration Fine	WT	12,587,757
RANS Full Configuration Fine	WT	25,175,514
Euler Full Configuration Coarse	XML1	191,736
Euler Full Configuration Fine	XML1	1,599,889

4. Aerodynamic Results

Wind tunnel data for the lift, drag and pitching moment coefficients is available at low speed [6]. The conditions of the wind tunnel tests were $U = 70$ m/s, $Re = 1.215$ million, $P_\infty = 100246.1$ Pa, and $T_\infty = 294.4$ K for a wind tunnel model with a wing span of 2.018m. The comparisons between the measurements, and the RANS and Euler predictions using the PMB solver applied to the WT geometry are shown in Fig. 4. The RANS results match the measurements well, with the exception of an overprediction of the drag at the higher angles. As expected, the lift coefficient is well predicted by the Euler equations also. The drag is shifted down when compared with the RANS predictions, reflecting the lack of the skin friction contribution. Neither DATCOM nor Euler predictions match the measured pitching moment slope due to differences in the drag force.

Euler predictions of drag, lift and pitching-moment coefficients are compared for the WT and XML1 geometries at transonic conditions in Fig. 5. In addition, the surface pressures for the XML1 model is compared with Euler WT and RANS WT results. The comparisons show the magnitudes of forces and moments for the two geometries are slightly different, but the trends of the predictions agree well. Note that the XML1 CAD model has generic aerofoil sections and lacks the refinements of the WT model like the fuselage/ wing junction blending. Given these differences, it is expected to see differences in the flow solutions. The overview of the flow solutions shows different stagnation regions at the nose, clearly related to the geometry difference in this region. There is also a small discrepancy in the junction between the nose section and the fuselage arising from the change in slope. More importantly, the flow around the wing root has significant differences. The leading edge at the root is thinner for the XML geometry, reducing the suction peak and the intensity of the shock wave. The flow towards the root then accelerates again for the XML geometry and produces another shock wave. At the mid-board and out-board sections of the wing, the WT aerofoil is thinner compared with XML1 (see Fig. 2-i), resulting in a weaker shock and less drag. In summary, the main differences between the forces and moments of the WT and XML geometries are associated with the wing geometry, and in particular the aerofoil section, rather than the lack of refinement of the XML geometry.

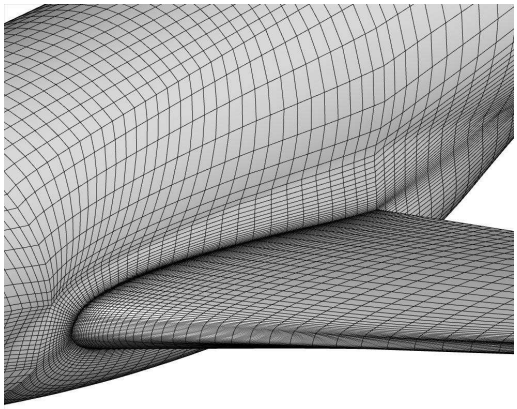

(a) WT

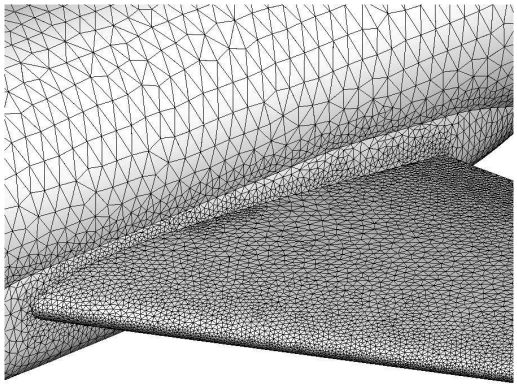

(b) XML1

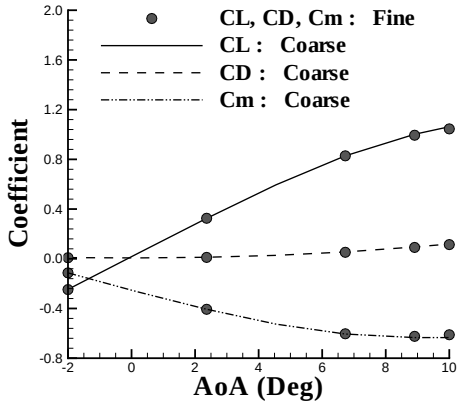

(c) XML1 grid refinement, predictions are at M=0.8 and zero side-slip angle.

Figure 3: Euler surface grids for the WT and XML1 geometries, and XML1 grid refinement study

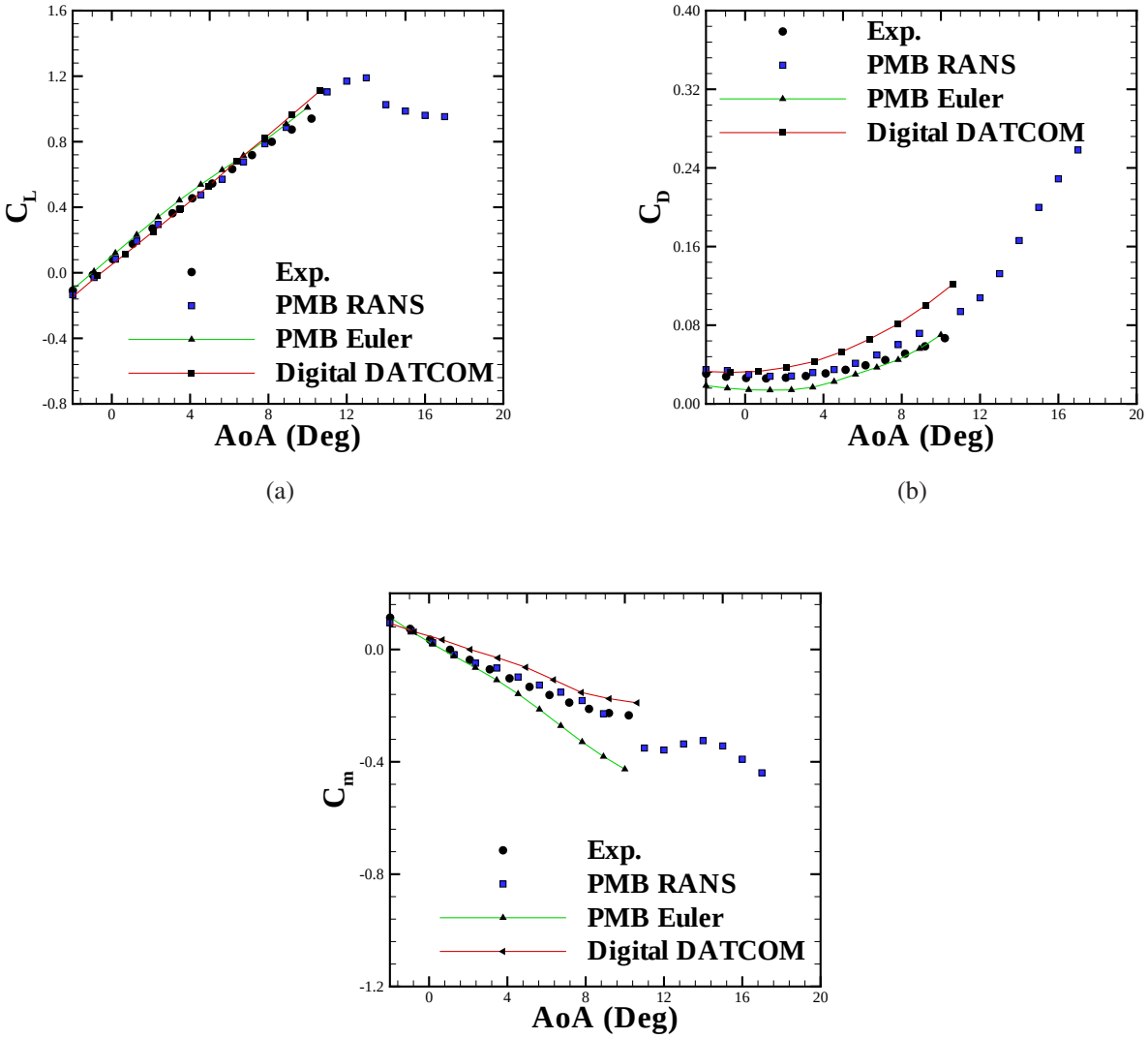

Figure 4: Comparison of PMB predictions for the WT Geometry at M=0.2

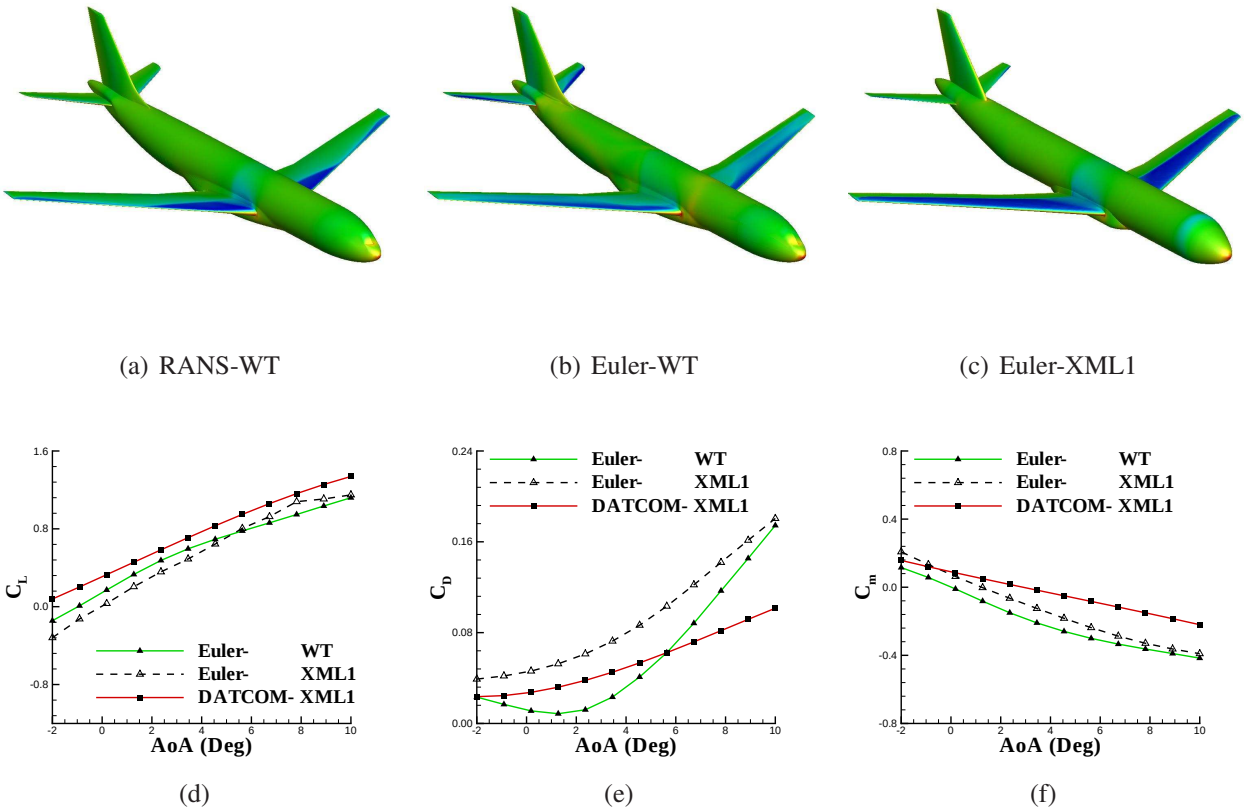

(a) RANS-WT (b) Euler-WT (c) Euler-XML1

(d) (e) (f)

Figure 5: Comparison of predictions for the WT and XML1 Geometry at M=0.8. Surface pressures correspond to AoA=8^0

5. Aerodynamic Tables

Sampling and data fusion is used to generate aerodynamic tables for the original conceptual geometry (XML1). The process followed was meant to mimic that of the first and second design scenarios described above.

The tables for this geometry were generated from scratch under the first scenario. A 648 entry, three-parameter table (angle of attack, Mach number and side-slip angle) was first generated using the Edge solver. Each calculation took one hour using a single processor. Sampling was used to define parameters for 65 calculations, and Kriging was then used to construct all of the table entries. The generated table describes the underlying behaviour of the XML1 aerodynamics. Sixteen test samples were generated at random flight conditions and the difference of values predicted from the table with those calculated by the Edge solver calculated. Small errors are obtained for all samples with the root mean square error for the lift coefficient being 0.0045 and for the pitching moment as 0.022304.

Next, the table for varying angle of attack, Mach number and elevator deflection was generated. Twelve additional samples at non-zero elevator angles were defined around the border of the table and in the nonlinear regimes highlighted by the first table. The values at these samples were then used to increment the original table values using Co-Kriging.

A number of geometry increments of the XML1 were defined and are shown in Fig. 6. Under the second design scenario, it is assumed that these geometries are increments of the XML1 geometry. This assumes that the flow regimes are the same, although the magnitudes of forces and moments are different. Then, 14 samples were defined (some at the border to avoid extrapolation and some at non-linear regions seen in the XML1 table) and calculated for the XML1 geometry using the Edge solver, and the XML1 table was updated using Co-Kriging. Again 16 test samples were defined at random and the difference of predictions from the table with CFD calculations is again small, with the Root Mean Square(RMS) error being 0.0019 for side-force coefficient (C_Y) and 0.044 for rolling moment(C_l).

A RANS-based aerodynamic table for varying angle of attack, Mach number and side-slip angle was generated for the WT geometry using the PMB solver under the second scenario. It is assumed that for angles of attack below stall, the RANS-based table is an increment of table of the XML1 geometry. Then, 20 samples were defined and calculated for the WT geometry using the PMB solver in RANS mode, and the angle of attack, Mach number and side-slip table for the XML1 geometry was updated using Co-Kriging. Each calculation was performed in 32 processors and took two hours for a full converged solution. To allow the tables with control surface effects to be generated for the WT geometry, it is assumed that the increment in the forces or moments arising from the control surface deflections is identical to that arising for the XML1 geometry.

6. Evaluation of Euler and DATCOM Predictions

Having generated aerodynamic tables, two issues need to be addressed. The first is to consider how designers can benefit from access to CFD data early in the design cycle. The second issue is whether the differences in forces and moments between the XML geometries reflect the different

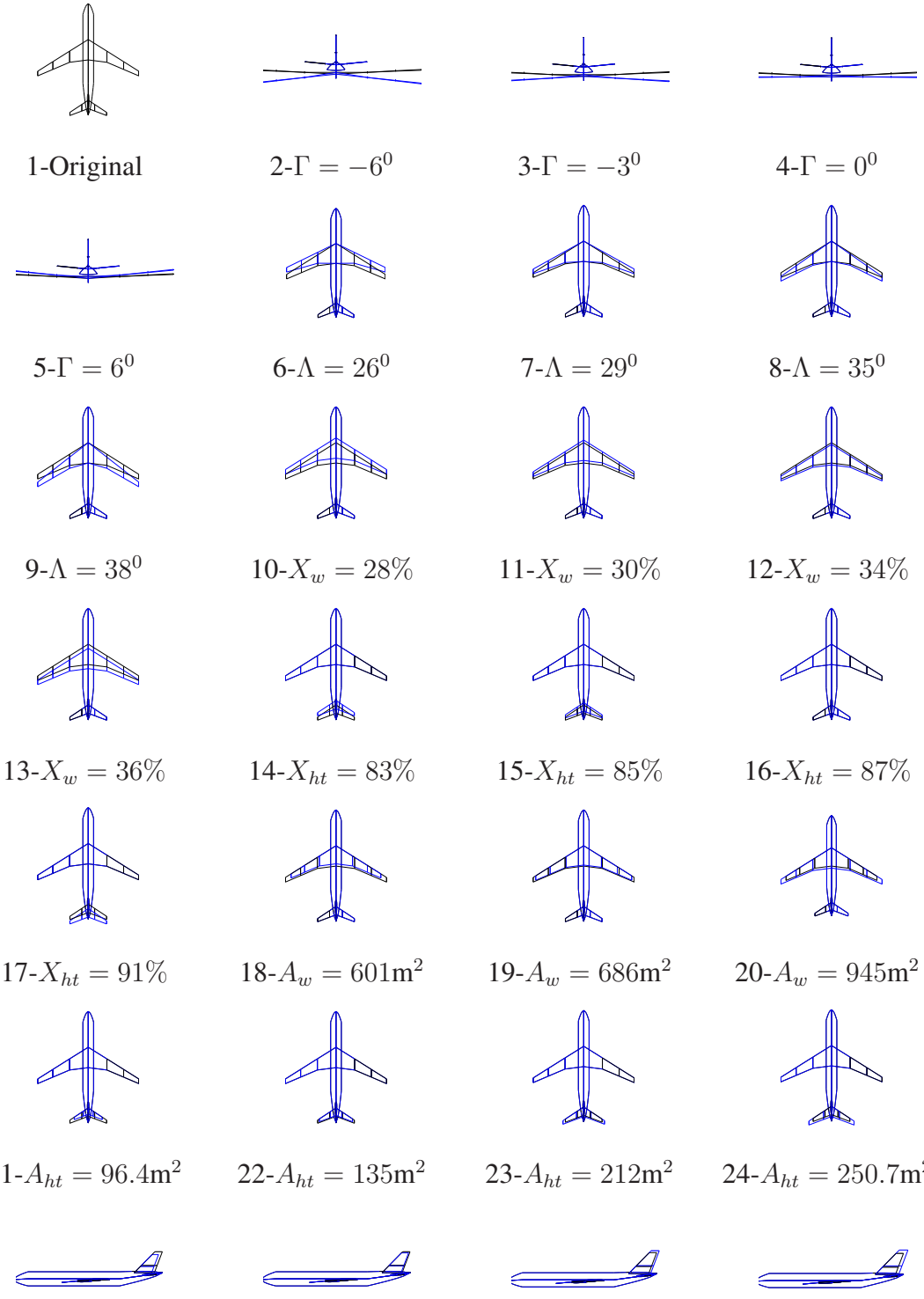

Figure 6: Geometry increments used for design study. The original is drawn with black colour

shapes, or are determined by artefacts from the lack of refinement in the geometry description. CFD has fewer limitations at transonic conditions than hand-book equations. Inspecting the aerodynamic tables for DATCOM and Euler at M=0.8 shows that DATCOM predicts significantly less drag (Fig. 5-f). The Euler results show a reduced lift curve slope and a change of pitching moment curve slope at high angles of attack as the shock moves towards the wing leading edge (Fig. 5-e, 5-g).

To consider the second issue, the aerodynamic predictions from DATCOM and Euler are compared. A large bank of experience for conventional aircraft is available in the literature for reference. The results show that for most features, the general trends of Euler and DATCOM agree well with limited differences:

- DATCOM and Euler show a falling trend of the rolling moment coefficient with respect to side-slip angle ($C_{l\beta}$) with increasing dihedral angle (Γ_w) (Fig. 7-a). This agrees with the expected trend, since Roskam [29] reports a negative increment of rolling moment for increasing dihedral angle at fixed wing root vertical placement.

- The rate of change of pitching moment coefficient with angle of attack ($C_{m\alpha}$) with increasing tail area (A_{HT}) is negative (Fig. 7-b). Again, this is what is expected since the aircraft aerodynamic centre moves aft as the horizontal tail increases.

- The rate of change of the yawing moment coefficient with side-slip angle ($C_{n\beta}$) with increasing fin area is positive for both DATCOM and Euler (Fig. 7-c) for similar reasons.

- The absolute value of yawing moment rudder control derivative ($C_{n\delta_r}$) increases as the fin area (A_{VT}) increases (Fig. 7-d). Roskam shows that there is a direct relationship with the fin area.

In two respects the flow models show different trends (Figs 7-e and 7-f). The variation of side-force coefficient with sideslip angle ($C_{y\beta}$) has contributions from the wing, fuselage, and vertical tail. Roskam [29] details the wing and fuselage contributions as:

$$C_{y_\beta w} = -0.00573 \times (|\Gamma|) \tag{6.1}$$

$$C_{y_\beta fuse} = -2 \times K_{wbi} A_o / A_w \tag{6.2}$$

where Γ denotes the wing dihedral and K_{wbi} is the wing-body interference factor. The latter term depends on Z_w, the distance between the body centreline and the quarter-chord point of the exposed wing root chord, positive for the quarter-chord point below the body centreline. For the fixed wing root vertical placement, Z_w will increase as the dihedral angle decreases, resulting in a larger wing-body interference factor and a further fall of C_{y_β} for negative dihedral angles. For positive dihedral angles, if the wing-body interference dominates the effects of C_{y_β}, then there is an increase in C_{y_β} with respect to dihedral angle. Fig. 7-e shows that the Euler solution estimates more wing-body interference compared with the semi-empirical K_{wbi} term used in DATCOM. The reason is

that DATCOM has no correction method for the estimation of the wing and body interference at transonic conditions.

The lift pitch rate derivative ($C_{Lq} + C_{L\dot{\alpha}}$) decreases as the *CG* shifts towards the aerodynamic centre. The Centre of Gravity *CG* and Aerodynamic Centre *AC* move aft as the wing sweep angle increases. However, the ratio of *AC* to *CG* movement is greater than one in DATCOM, and less than one for Euler. The reason is that due to DATCOM limitations, the actual wing is described by an equivalent straight-tapered geometry. This results in an increasing trend of $C_{Lq} + C_{L\dot{\alpha}}$ with respect to the wing sweep angle(Fig. 7-f).

In summary, DATCOM aerodynamic tables fail to fully predict the effects of transonic conditions on aerodynamic forces and moments. There are also limitations arising from describing the aircraft geometry in DATCOM: the fairing is not considered, dynamic derivatives are only predicted for the straight-tapered wing, the effects of twist is considered at subsonic Mach numbers, whereas the Euler aerodynamic tables based on the computer-aided concept design has no limitations related to the geometry. Since DATCOM is based on a database for conventional aircraft, the situation for novel configurations is likely to be worse.

7. Flight Handling Qualities

To calculate handling qualities, the *CG* position, mass and moments of inertia need to be estimated. In this paper, these are obtained from CEASIOM based on semi-empirical methods given in aircraft design books [25] and [29].

The generated aerodynamic look up tables are fed to the flight simulation module, SDSA. For eigenvalue analysis a non-linear model is linearized numerically using the Jacobian matrix of the state derivatives around the trim point. Figures of merits based on aircraft regulations, the flight control model and trim analysis are all available. The aerodynamic responses to perturbation of control surfaces from the trim point are characterized by the undamped natural frequency(ω) or period (T), damping ratio (ζ) and time to half amplitude($T_{\theta 2}$).

Figures 8-a to 8-c show the comparison of values of the angle of attack, elevator deflection and thrust for trimming the XML1 model for a range of flight speeds at 6,000m altitude. The predictions based on the Euler generated aerodynamics result in a smaller elevator deflection angle compared with DATCOM. This is due to the different pitching moment curve slope for CFD simulations at transonic conditions. Also, the increase of drag force results in an increased required thrust as the flight speed increases.

The SDSA code, using the supplied aerodynamic tables, calculates the aircraft flight handling figures of merit. Here, the results concerning the Phugoid, based on the International Civil Aviation Organization(ICAO) opinion-contour graph, and using a Cooper-Harper rating scale, is shown in Fig. 8-d. There is a large discrepancy in Phugoid characteristics between using the Euler and DATCOM aerodynamic tables at high speed. This arises from the Euler drag and pitching-moment increases at transonic speeds. The Phugoid attributes improve with increasing flight speed for all of the aerodynamic sources (as shown in Fig. 8-d), but DATCOM predicted value is poor. The aircraft natural frequencies are too small when using the DATOCM aerodynamic tables. The Short-period

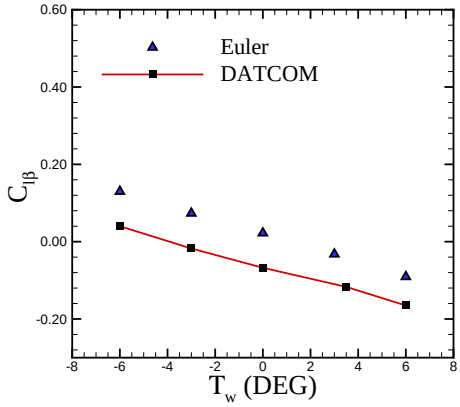

(a)

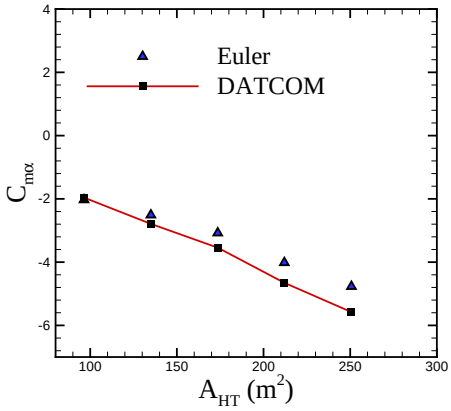

(b)

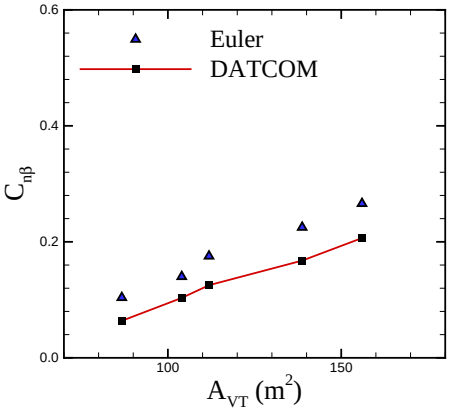

(c)

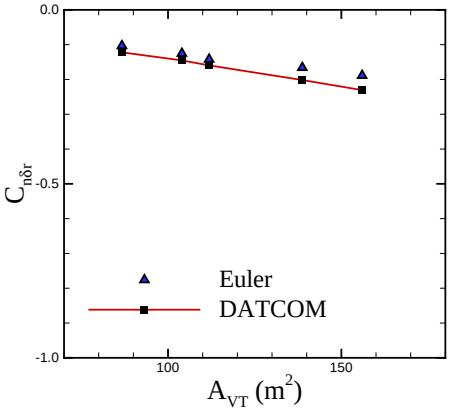

(d)

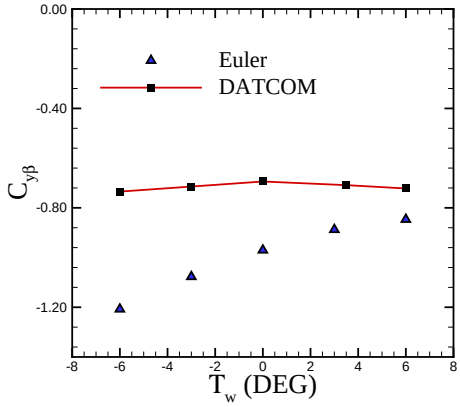

(e)

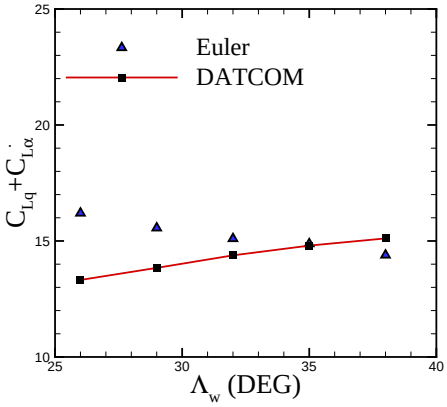

(f)

Figure 7: Aerodynamic derivatives predictions from DATCOM and Euler. In all cases, AoA= 0.0^o, M= 0.8

characteristics are also shown in Figs. 8-e - 8-f. The results are based on the Euler and DATCOM tables for the XML1, in conjunction with RANS tables for the WT geometry, obtained for an altitude of 6,000 m and two flight speeds of V=200 m/s and V=300 m/s. The figures show that DATCOM results are less satisfactory and controllable compared with those found for Euler. This is a direct result of the DATCOM predicted natural frequency being too small.

Next the impact of geometry increments on the handling qualities is investigated. The influence of the wing area and sweep angle on the Short-period mode are seen in Fig. 9, where the results have been plotted in an ICAO opinion-contour graph. The flight conditions correspond to V=300 m/s and altitude of 6,000 m. The period mainly depends on the pitching moment curve slope, while, the time to half amplitude is also influenced by the aircraft pitch damping. The predictions include the effect of changes in the moments of inertia and the aircraft mass.

The results show that the CFD based aerodynamic tables provide better understanding of the vehicle handling qualities at transonic conditions, whereas, the tables from DATCOM are misleading. Using CFD for the conceptual aircraft design is a key step towards both minimizing the costly geometry modifications after the conceptual phase, and including control design more explicitly earlier in the design cycle.

8. Conclusions

The results in this paper demonstrate that the automated calculation of flight handling qualities of a conceptual aircraft design is now possible using physics based aerodynamic simulation data. The steps that allow this are (a) the automated generation of meshes for Euler calculations around complete aircraft starting from a high level conceptual definition of the geometry; (b) fast generation of aerodynamic tabular models based on sampling and data fusion and (c) the coupling of these tools with an analysis code for flight dynamics. Results were presented to benchmark and assess the impact of the geometry definition on the Euler calculations, to compare the predictions of different aerodynamic modelling levels on handling quality predictions, and to show that the expected trends from changing geometry parameters are obtained.

Future work will go in two directions. First, the opportunity is now there to exploit simulation for driving control design at the conceptual stage. It is expected that this will enable the consideration of a wider range of potential designs, with the use of active control to remove previously insurmountable obstacles arising from the geometry. Secondly, the extension of the automated analysis to include RANS simulations poses the challenge of automatically generating suitable meshes, and revisiting the impact of geometry roughness when flow separation is possible.

Acknowledgements

Liverpool was supported under funding from the Sixth Framework programme of the European Union for the SimSAC project, and the Engineering and Physical Sciences Research Council and the Ministry of Defence under EP/D504473/1. KTH was supported by the SimSAC project. Multiblock structured Euler and RANS grids were generated by CERFACS for the WT geometry.

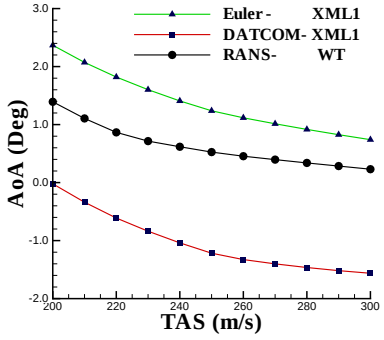

(a) Trim- Angle of Attack

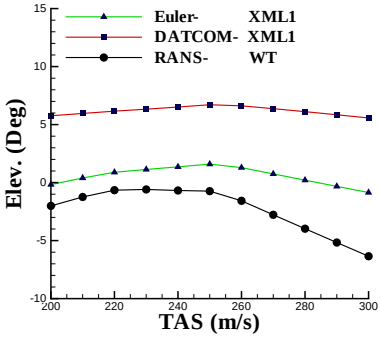

(b) Trim- Elevator Deflection

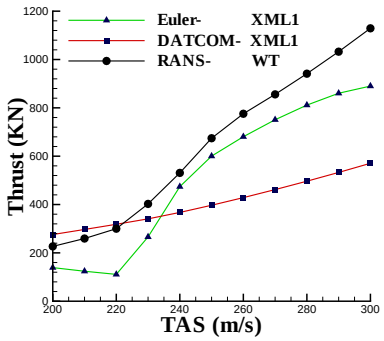

(c) Trim- Required Thrust

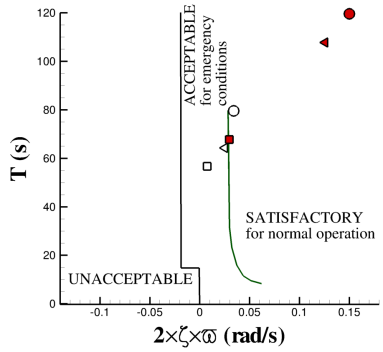

(d) ICAO opinion-contour graph for Phugoid Characterizes

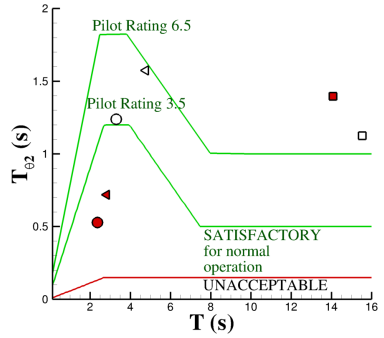

(e) ICAO opinion-contour graph for Short-Period Characterizes

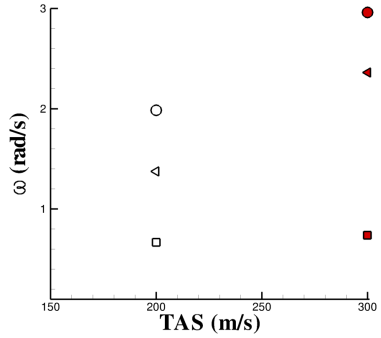

(f) Short-Period Undamped Natural Frequency

Figure 8: XML1 Trim and Handling qualities at altitude 6000 m- In subfigures (d)-(f), XML1 DATCOM and Euler are denoted by squares and left triangle symbols, respectively. WT RANS results are shown with circles. The filled symbols show V= 300 m/s, while the non-filled ones show V= 200 m/s

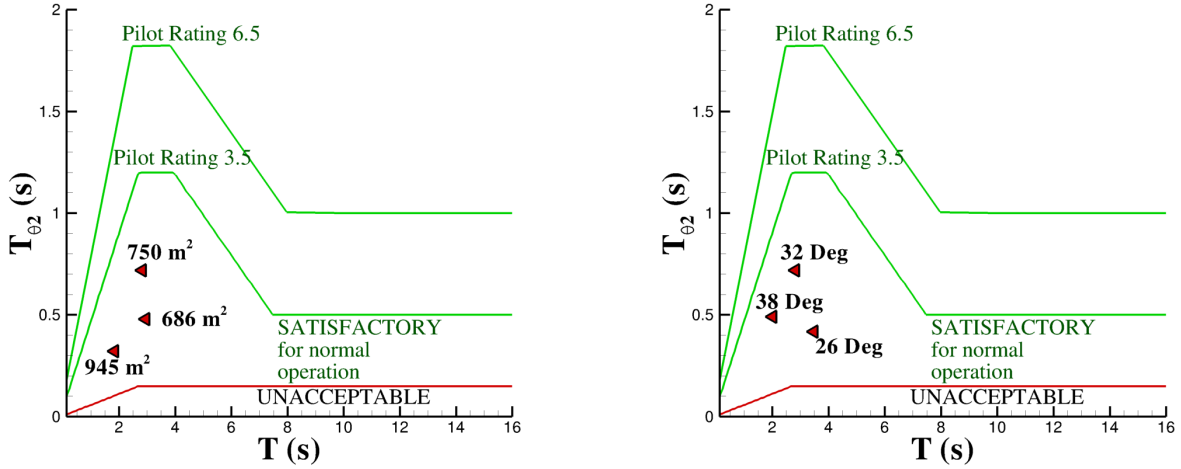

(a) Wing Area Influence

(b) Wing Sweep Angle Influence

Figure 9: Effects of Design into short period characteristics. Results are based on the Euler tables at an altitude of 6000 m and V= 300 m/s. The results include the effects of *CG*, mass and moments of inertia variation

Computer time for the RANS calculations was provided though the UK Applied Aerodynamics Consortium (UKAAC) under EPSRC grant EP/F005954/1.

References

[1] J. J. Alonso, J. R. Martins, J. J. Reuther, R. Haimes, C. A. Crawford. *High-fidelity aero-structural design using a parametric CAD-based model*.16th AIAA Computational Fluid Dynamics Conference, Orlando, FL, June 23- 26, 2003, AIAA-2003-3429.

[2] K. J. Badcock, B. E. Richards, M. A. Woodgate. *Elements of computational fluid dynamics on block structured grids using implicit solvers*. Progress in Aerospace Sciences, 36 (2000), 351–392.

[3] J. T. Baker. *Mesh generation: Art or science*? Progress in Aerospace Sciences, 41 (2005), 29–63.

[4] K. Becker, J. Vassberg. *Numerical aerodynamics in transport aircraft design*. Notes on Num. Fluid Mechanics, 100 (2009), 209–220.

[5] A. Berard, A. Rizzi, A. T. Isikveren. *CADac: a new geometry construction tool for aerospace vehicle pre-design and conceptual design*. 26th Applied Aerodynamics Conference, Honolulu, Hawaii, USA, August 18-21, 2008, AIAA-2008-6219.

[6] A. Bergmann, A. Hubner, T. Loeser. *Experimental and numerical research on the aerodynamics of unsteady moving aircraft*. Progress in Aerospace Sciences, 44 (2008), 121–137.

[7] W. B. Blake. *Prediction of Fighter Aircraft Dynamic Derivatives Using Digital Datcom*. AlAA 3^{rd} Applied Aerodynamics Conference, Colorado Springs, Colorado, October 14-16, 1985, AIAA-85-4070.

[8] K. Bowcutt. *A perspective on the future of aerospace vehicle design*. 12th AIAA International Space Planes and Hypersonic Systems and Technologies, Norfolk, Virginia, Dec. 15-19, 2003, AIAA 2003-6957.

[9] G. E. Cooper. *Understanding and interpreting pilot opinions*. Aeron Eng. Rev., 16 (1957), No. 3, 47–51.

[10] P. Eliasson. EDGE, a Navier-Stokes solver for unstructured grids, finite volumes for complex applications III: problems and perspectives. Hermes Penton Science, London, 2002.

[11] J. R. Gloudemans, P. C. Davis, P. A. Gelhausen. *A rapid geometry modeler for conceptual aircraft*. 34th Aerospace Sciences Meeting and Exhibit, Reno, NV, Jan. 15-18, 1996, AIAA-1996-0052.

[12] T. Goetzendorf-Grabowski, J. B. Vos, S. Sanchi, P. Molitor, M. Tomac, A. Rizzi. *Coupling adaptive-fidelity CFD with S&C analysis to predict flying qualities*. 27th AIAA Applied Aerodynamics Conference, San Antonio, Texas, June 22-25, 2009, AIAA-2009-3630.

[13] M. Ghoreyshi, K. J. Badcock, M. A. Woodgate. *Accelerating the numerical generation of aerodynamic models for flight simulation*. Journal of Aircraft, 46 (2009), No. 3, 972–980.

[14] R. Haimes. CAPRI: Computational analysis programming interface. CAPRI technical guide, Massachusetts Institute of Technology, 1998.

[15] A. T. Isikveren. Quasi-analytical modelling and optimisation techniques for transport aircraft design. PhD Thesis, Department of Aeronautics, Royal Institute of Technology, Stockholm, Sweden, 2002.

[16] R. von Kaenel, A. Rizzi, J. Oppelstrup, T. Goetzendorf-Grabowski, M. Ghoreyshi, L. Cavagna, A. Berard. *CEASIOM: simulating stability & control with CFD/CSM in aircraft conceptual design*, 26th International Congress of the Aeronautical Sciences, ICAS, 2008.

[17] F. Ladeinde. *Truely automatic CFD mesh generation with support for reverse engineering*. Aerospace Sciences Meeting and Exhibit, 37th, Reno, NV, Jan. 11-14, 1999, AIAA 99-0828.

[18] R. Lohner. *Automatic unstructured grid generators*. Journal of Finite Elements in Analysis and Design, 25 (1997), 111–134.

[19] R. Lohner, J. Cebral. *Generation of non-isotropic unstructured grids via directional enrichment*. International Journal for Numerical Methods in Engineering, 49 (2000), 219-232.

[20] W. H. Mason, D. L. Knill, A. A. Giunta, B. Grossman, L. T. Watson, R. T. Haftka. *Getting the full benefits of CFD in conceptual design.* 16th Applied Aerodynamics Conference, Albuquerque, NM, June 15-18, 1998, AIAA 98-2513.

[21] D. N. Mavris, D. A. DeLaurentis, D. S. Soban. *Probabilistic assessment of handling qualities characteristics in preliminary aircraft design*. 36th Aerospace Sciences Meeting and Exhibit, Reno, NV, Jan. 12-15, 1998, AIAA 98-0492.

[22] B. Mialon, S. Ben Khelil, A. Huebner, J.-C. Jouhaud, G. Roge, S. Hitzel, K. Badcock, P. Eliasson, A. Khabrov, M. Lahuta. *European benchmark on numerical prediction of stability and control derivatives*. 27th AIAA Applied Aerodynamics Conference, San Antonio, TX, June 22-25, 2009, AIAA-2009-4116.

[23] D. J. McCormick. An analysis of using CFD in conceptual aircraft design, M.S. Thesis, Dept. of Mechanical Engineering, Virginia Polytechnic Institute, Blacksburg, VA, 2002.

[24] T. Melin, A. T. Isikveren, A. Rizzi, C. Stamblewski, H. V. Anders. *How industry concepts of concurrent engineering enhance aircraft design education*. Journal of Aerospace Engineering, 221 (2007), 175–192.

[25] D. P. Raymer. Aircraft design: A conceptual approach. AIAA Education Series, Reston, VA, USA, 2006,

[26] V. Razgonyaev, W. H. Mason. *An evaluation of aerodynamic prediction methods applied to the XB-70 for use in high speed aircraft stability and control system design*. 33rd Aerospace Sciences Meeting and Exhibit, Reno, Nevada, 1995, AIAA-95-0759.

[27] S. E. Rogers, M. J. Aftomis, S. A. Pandya, N. M. Chaderjian, E. T. Tejnil, J. U. Ahmad. *Automated CFD parameter studies on distributed parallel computers*. 16th AIAA Computational Fluid Dynamics Conference, Orlando, Florida, 2003, AIAA 2003-4229.

[28] D. L. Rodriguez, P. Sturdza. *A rapid geometry engine for preliminary aircraft design*. 44th Aerospace Science Meeting and Exhibit, Reno, NV, Jan. 9-12, 2006, AIAA-2006-929.

[29] J. Roskam. Airplane design. Roskam Aviation and Engineering Corporation, Kansas, USA, 1990.

[30] J. E. Williams, S. R. Vukelich. The USAF stability and control digital DATCOM. McDonnell Douglas Astona UTICS Company, St Louis Division, St Louis, Missouri, AFFDL-TR-79-3032, 1979.